Frascati Physics Series Vol. LVI (2012)
Dark Forces at Accelerators
October 16-19, 2012

U boson search in ϕ Dalitz decays with KLOE

I. Sarra on behalf of the KLOE-2 collaboration
Laboratori Nazionali di Frascati, INFN, Frascati, Italy

Abstract

We have carried out a new search for the existence of a light dark force mediator with the KLOE detector at DAΦ NE. This particle, called U, has been looked for by adding to the already used $\phi \to \eta U$, $\eta \to \pi^+\pi^-\pi^0$ and $U \to e^+e^-$, the same decay chain with $\eta \to \pi^0\pi^0\pi^0$. The latter sample (1.7 fb^{-1}) results to have better reconstruction efficiency and reduced background contamination than the previously used sample (1.5 fb^{-1}). No structures are observed in the e^+e^- invariant mass distribution over the background. The resulting exclusion plot, obtained by combining both samples with CLS method, covers the mass range $5 < M_U < 470$ MeV and sets an upper limit at 90% C.L. on the ratio between the U boson coupling constant and the fine structure constant, α'/α, of $\leq 1.7 \times 10^{-5}$ for $30 < M_U < 400$ MeV and $\leq 8.0 \times 10^{-6}$ for $50 < M_U < 210$ MeV. This result assumes the Vector Meson Dominance expectations for the $\phi\eta\gamma^*$ transition form factor. The dependence of this limit on the transition form factor has also been studied.

1 Anomalous experimental results and their possible explanation

A variety of astrophysical observations indicate that 83% of the matter in the Universe is non baryonic and dark, presumably in the form of elementary particles produced in the early Universe. Since no such particles have yet been identified in particle accelerators, these observations require new fundamental particle physics.
Moreover, recent experiments have confirmed the longstanding suspicion that there are more positrons and electrons at 10-100 GeV than can be explained by supernova shocks and interactions of cosmic ray protons with the Interstellar Medium (ISM). The experiments are:

- **Pamela:** The Payload for Antimatter Matter Exploration and Light-nuclei Astrophysics has reported results [1)] indicating a sharp upturn in the positron fraction $(e^+/(e^+ + e^-))$ from $10-100$ GeV, contrary to what expected from high-energy cosmic rays interacting with the interstellar medium IMS. One possible explanation for this is dark matter annihilation into $e^- e^+$.

- **Fermi:** The Fermi Gamma-Ray Telescope can distinguish more than gamma rays. It has now provided the most accurate measurement of the spectrum of cosmic-ray electrons and positrons. These results are consistent with a single power law, but visually they suggest an excess emission from about 100 GeV to 1 TeV [2)]. The additional source of electrons and positrons could come from nearby pulsars or dark matter annihilation. Dark matter would seem a natural candidate for this as well, with its mass scale determining the cutoff.

- **Integral:** The INTEGRAL satellite [3)] observes a 511 keV signal from the galactic core, which suggests the existence of an abundant positron annihilation source, far exceeding what expected from supernovae only.

If we focus only on the high-energy positrons and electrons, there are a number of challenges to any model of dark matter. PAMELA and FERMI signals require a cross section much larger than what allowed by the thermal relic abundance. Boost factors of O(100) or more above what would be expected for a thermal WIMP are required to explain these excesses [4)]. Moreover:

- *A large cross section into leptons*: typical annihilations via Z bosons produce very few hard leptons. Annihilations into W bosons produce hard leptons, but many more soft leptons through the hadronic shower. Higgs bosons and heavy quarks produce even softer spectra of leptons, all of which seem to give poor fits to the data. At the same time, absent a leptonic gauge boson, it is a challenge to construct means by which dark matter would annihilate directly to leptons.

- *A low cross section into hadrons*: Even if a suitably high annihilation rate into leptons can be achieved, the annihilation rate into hadronic modes must be low. PAMELA measurements of antiprotons tightly constrain hadronic annihilations as well. Consequently, although quark and gauge boson annihilation channels may occur at some level, the dominant source of leptons must arise through some other channel.

The combination of these issues makes the observed high-energy anomalies difficult to explain with thermal dark matter annihilation. However, the inclusion of a new force in the dark sector simultaneously addresses all of these concerns. It is postulated the existence of relatively heavy (~ 1 TeV) Weakly Interacting Massive Particles (WIMPs) states together with at least one relatively light ($\sim$ 1 GeV) vector boson, mediator of a new hidden gauge symmetry.
Although SM particles are not charged under this new symmetry they can still couple with the dark photon through the kinetic mixing mechanism with ordinary SM bosons, and specifically with the photon. The Lagrangian is of the form:

$$\mathcal{L} = \mathcal{L}_{SM} + \mathcal{L}_{Dark} + \mathcal{L}_{mix} \tag{1}$$

where

$$\begin{aligned} \mathcal{L}_{Dark} = \mathcal{L}^{F}_{Dark}(X) &\quad \Rightarrow \quad M_X \sim 100 - 1000\, GeV \;\; WIMP \\ +\mathcal{L}^{B}_{Dark}(U) &\quad \Rightarrow \quad m_U \sim GeV \;\; U\ Boson \\ +\mathcal{L}^{B}_{Dark}(h') &\quad \Rightarrow \quad higgs\ potential\ breaking\ U(1)_D \end{aligned}$$

Typically, the mixing strength is parametrized by a single parameter ϵ_D, whose value has to be determined experimentally. However, in order to better

accommodate the above mentioned experimental results, preferred values of ϵ_D are in the ball-park of 10^{-3}. As a consequence of that, the U can be produced and observed at present day colliders depending on its mass and on the value of ϵ_D, as discussed in the next sections.

2 The KLOE detector

DAΦ NE, the Frascati ϕ-factory, is an e^+e^- collider running at center-of-mass energy of ~ 1020 MeV. Positron and electron beams collide at an angle of π-25 mrad, producing ϕ mesons nearly at rest. The KLOE experiment operated at this collider from 2000 to 2006, collecting 2.5 fb^{-1}. The KLOE detector consists of a large cylindrical Drift Chamber (DC), surrounded by a lead-scintillating fiber electromagnetic calorimeter (EMC), all embedded inside a superconducting coil, providing a 0.52 T axial field. The beam pipe at the interaction region is a sphere with 10 cm radius, made of a 0.5 mm thick Beryllium-Aluminum alloy. The drift chamber [6], 4 m in diameter and 3.3 m long, has 12,582 all-stereo tungsten sense wires and 37,746 aluminum field wires, with a shell made of carbon fiber-epoxy composite with an internal wall of ~ 1 mm thickness. The gas used is a 90% helium, 10% isobutane mixture. The momentum resolution is $\sigma(p_\perp)/p_\perp \approx 0.4\%$. Vertices are reconstructed with a spatial resolution of $\sim$ 3 mm. The calorimeter [7], with a readout granularity of $\sim(4.4 \times 4.4)$ cm^2, for a total of 2440 cells arranged in five layers, covers 98% of the solid angle. Each cell is read out at both ends by photomultipliers, both in amplitude and time. The energy deposits are obtained from the signal amplitude while the arrival times and the particles positions are obtained from the time differences. Cells close in time and space are grouped into energy clusters. Energy and time resolutions are $\sigma_E/E = 5.7\%/\sqrt{E\ (\mathrm{GeV})}$ and $\sigma_t = 57$ ps$/\sqrt{E\ (\mathrm{GeV})} \oplus 100$ ps, respectively. The trigger [8] uses both calorimeter and chamber information. In this analysis the events are selected by the calorimeter trigger, requiring two energy deposits with $E > 50$ MeV for the barrel and $E > 150$ MeV for the endcaps. Data are then analyzed by an event classification filter [9], which selects and streams various categories of events in different output files.

3 Searches for a U Boson mediator

The astrophysical observations suggest the existence of a WIMP dark matter particle and of a secluded gauge sector $U(1)_D$ under which the SM particles are uncharged. The abelian gauge field weakly interacts with the $U(1)_Y$ of the SM4 by an invariant kinetic mixing term:

$$\Delta\mathcal{L} = \epsilon_D F^{Y,\mu\nu} F_{D,\mu\nu} \tag{2}$$

The mixing parameter ϵ is of the order of 10^{-4} - 10^{-2}. The Feynman diagram is showed in figure 1. The vector boson U has mass near the GeV scale.

Figure 1: The U boson can communicate with the SM through a kinetic mixing term describing the interaction of the U boson with SM photon. In this case the parameter ϵ_D should be smaller than 10^{-2}.

These hypothesis lead to the consequence that observable effects can be induced in $\mathcal{O}$(GeV) energy e^+e^- colliders such as DAΦNE or present and/or future B factories. The U boson can be also produced in electron collisions on a fixed target, such as MAMI [16], in a process analogous to ordinary bremsstrahlung. In this case, production cross sections are much higher with respect to e^+e^- processes. However backgrounds, both from ordinary QED reactions and from possible beam related sources are also higher.
The U boson can be produced in e^+e^- collisions via the radiative reaction $e^+e^- \to U\gamma$, with subsequent decay of the U into a lepton pair. If the two leptons are charged, the U can be observed as a resonant peak of the lepton pair invariant mass distribution over the standard continuous QED background.
A further line of search available at e^+e^- colliders is the study of the decays of a vector meson into a pseudo-scalar and a U, as suggested by Reece and Wang [10]. This decays should occur at a rate suppressed by a factor ϵ with respect to the standard radiative ones, which have typical branching ratios of $\sim$

1%. In particular Reece and Wang have focussed their attention on the channel $\phi(1020) \to \eta U$. With the statistics acquired so far by the KLOE experiment at the DAΦNE facility in Frascati, they have argued that one could probe mixing parameters down to 10^{-3}, for U masses below $m_\phi - m_\eta \sim 470$ MeV. This search has actually been performed by the KLOE-2 Collaboration, as described in the remaining of this paper.

4 Event selection

To improve the search for the U boson, we have carried out the analysis of the process $\phi \to \eta U$, $U \to e^+e^-$, adding the decay channel $\eta \to \pi^0\pi^0\pi^0$ to the previously used, $\eta \to \pi^+\pi^-\pi^0$. The new search has been performed on a data sample of 1.7 fb^{-1}, corresponding approximately to 6×10^9 produced ϕ mesons. The Monte Carlo (MC) simulation for the $\phi \to \eta U$ decay has been developed according to [10], with a flat distribution in the e^+e^- invariant mass, M_{ee}, while the irreducible background $\phi \to \eta e^+e^-$, $\eta \to \pi\pi\pi$, has been simulated according to a Vector Meson Dominance parametrization [11]. All MC productions, including all other ϕ decays, take into account changes in DAΦNE operation and background conditions on a run-by-run basis. Corrections for data-MC discrepancies in cluster energies and tracking efficiency, evaluated with radiative Bhabha scattering and $\phi \to \rho\pi$ event samples, respectively, have been applied.

As a first analysis step for the neutral η decay channel, a preselection is performed requiring:

1. two opposite charge tracks with point of closest approach to the beam line inside a cylinder around the interaction point (IP), of 4 cm transverse radius and 20 cm length;

2. six prompt photon candidates, *i.e.* energy clusters with $E > 7$ MeV not associated to any track, in an angular acceptance $|\cos\theta_\gamma| < 0.92$ and in the expected time window for a photon ($|T_\gamma - R_\gamma/c| < \mathrm{MIN}(3\sigma_t, 2\,\mathrm{ns})$);

3. a loose cut on the six-photon invariant mass: $400 < M_{6\gamma} < 700$ MeV.

After this selection, a peak corresponding to the η mass is clearly observed in the distribution of the recoil mass against the e^+e^- pair, $M_{\mathrm{recoil}}(ee)$ (Fig. 2). The second peak at ~ 590 MeV is due to $K_S \to \pi^+\pi^-$ decays with wrong

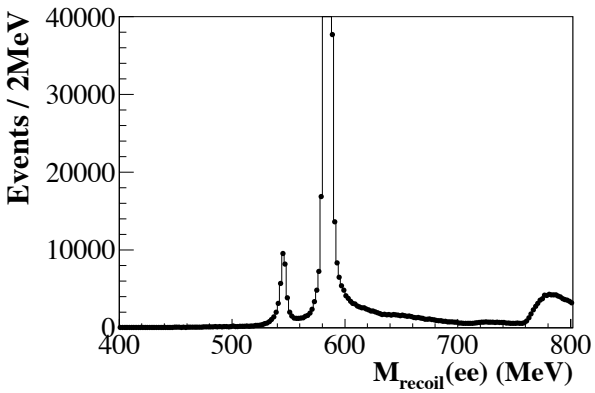

Figure 2: Recoiling mass against the e^+e^- pair for the data sample after preselection cuts. The $\phi \to \eta\, e^+e^-$ signal is clearly visible as the peak corresponding to the η mass.

mass assignment. To select $\phi \to \eta\, e^+e^-$ events, a 3σ cut is applied on this variable, $536.5 < M_{\rm recoil}(ee) < 554.5$ MeV. The retained sample has $\sim 20\%$ residual background contamination, constituted by $\phi \to \eta\gamma$, $\phi \to K_S K_L$ and $e^+e^- \to \omega\pi^0$ (about 50%, 35% and 15% of the whole background contribution, respectively). In Fig. 3, the comparison between data and Monte Carlo events for the M_{ee} and $\cos\Psi^*$ distributions is shown at this analysis level. The Ψ^* variable is the angle between the directions of the η and the e^+ in the e^+e^- rest frame. Photon conversion events are concentrated at $M_{ee} \sim 30$ MeV and $\cos\Psi^* < 0.6$, while the other backgrounds cover the $M_{ee} > 300$ MeV region and are uniformly distributed in $\cos\Psi^*$.

The $\phi \to \eta\gamma$ background contamination is mainly due to events where a photon converts to an e^+e^- pair on the beam pipe (BP) or drift chamber walls (DCW). After tracing back the tracks of the two e^+/e^- candidates, these events are efficiently rejected by reconstructing the invariant mass (M_{ee}) and the distance (D_{ee}) of the track pair both at the BP and DCW surfaces. Both variables are expected to be small for photon conversion events, so that this

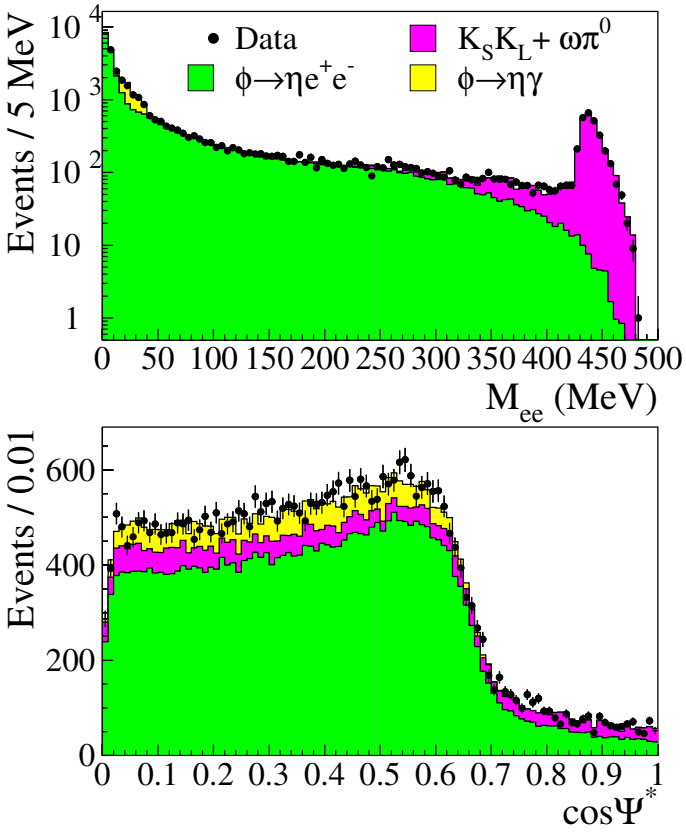

Figure 3: $\phi \to \eta\, e^+e^-$, $\eta \to \pi^0\pi^0\pi^0$ events: data-MC comparison for M_{ee} (top) and $\cos\Psi^*$ distributions (bottom) after the $M_{\rm recoil}(ee)$ cut.

background is removed by rejecting events with: [$M_{ee}(BP) < 10$ MeV and $D_{ee}(BP) < 2$ cm] or [$M_{ee}(DCW) < 120$ MeV and $D_{ee}(DCW) < 4$ cm].

At this stage of the analysis, the surviving background is dominated by events with two charged pions in the final state, and it is rejected by exploiting the timing capabilities of the calorimeter. When an energy cluster is associated to a track, the time of flight (ToF) to the calorimeter is evaluated both using

the track trajectory ($T_{\rm track} = L_{\rm track}/\beta c$) and the calorimeter timing ($T_{\rm cluster}$). The $\Delta T = T_{\rm track} - T_{\rm cluster}$ variable is then evaluated in the electron hypothesis (ΔT_e). In order to be fully efficient on signal, events with either an e^+ or an e^- candidate inside a 3σ window around $\Delta T_e = 0$ are retained for further analysis.

At the end of the analysis chain, 30577 events are selected, with $\sim 3\%$ background contamination (Fig. 4). The analysis efficiency, defined as the ratio between events surviving analysis cuts and generated events, is $\sim 15\%$ at low e^+e^- invariant masses, increasing up to 30% at higher M_{ee} values.

The analysis of the decay channel $\eta \to \pi^+\pi^-\pi^0$ is the same as described in [12], with the addition of a cut on the recoil mass to the $e^+e^-\pi^+\pi^-$ system, which is expected to be equal to the π^0 mass for signal events. In Fig. 5 top, data-MC comparison shows some residual background contamination in the tails of the distribution, which are not well described by our simulation. A cut $100 < M_{\rm recoil}(ee\pi\pi) < 160$ MeV is then applied. The effect of this cut on the M_{ee} variable is shown in Fig. 5 bottom. The total number of selected events is 13254, with $\sim 2\%$ background contamination.

5 Upper limit evaluation on U boson production

The upper limit on the U boson production in the $\phi \to \eta U$ process is obtained combining the two η decay channels. The resolution of the e^+e^- invariant mass has been evaluated with a Gaussian fit to the difference between the reconstructed and generated mass for Monte Carlo events, providing $\sigma_{M_{ee}} \leq 2$ MeV over the whole M_{ee} range. The determination of the limit is done by varying the M_U mass, with 1 MeV step, in the range between 5 and 470 MeV. Only five bins (5 MeV width) of the reconstructed M_{ee} variable, centered at M_U are considered. For each channel, the irreducible background, $b(M_U)$, is extracted directly from our data after applying a bin-by-bin subtraction of the non-irreducible backgrounds and correcting for the analysis efficiency. The M_{ee} distribution is then fit, excluding the bins used for the upper limit evaluation. The parametrization of the fitting function has been taken from Ref. [11]. The $\phi\eta\gamma^*$ transition form factor is parametrized as

$$F_{\phi\eta}(q^2) = \frac{1}{1 - q^2/\Lambda^2} \tag{3}$$

with $q = M_{ee}$. Free parameters are Λ and a normalization factor. The spread of the extracted parameters is contained within the statistical error of the fit

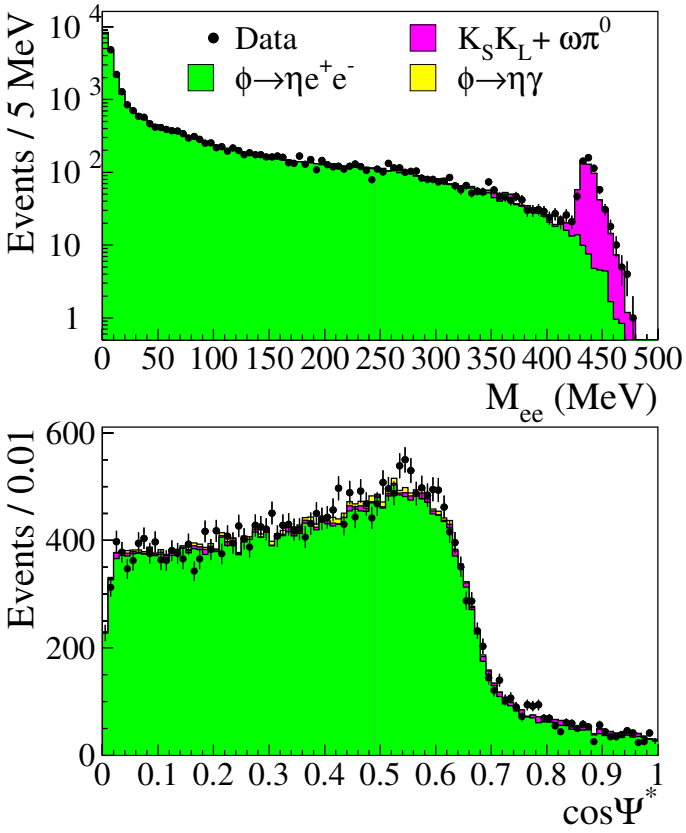

Figure 4: $\phi \to \eta\, e^+e^-$, $\eta \to \pi^0\pi^0\pi^0$ events: data-MC comparison for M_{ee} (top) and $\cos\Psi^*$ distributions (bottom) at the end of the analysis chain.

done on the whole M_{ee} mass range, shown in Fig. 6, as expected from the overall good description of the M_{ee} shape for both η decay channels.

The exclusion limit on the number of events for the $\phi \to \eta U$ signal as a function of M_U is obtained with the CL_S technique [13], using the M_{ee} spectra before background subtraction. The limit is extracted both for each η decay channel and in a combined way. For the combined procedure, the CL_S

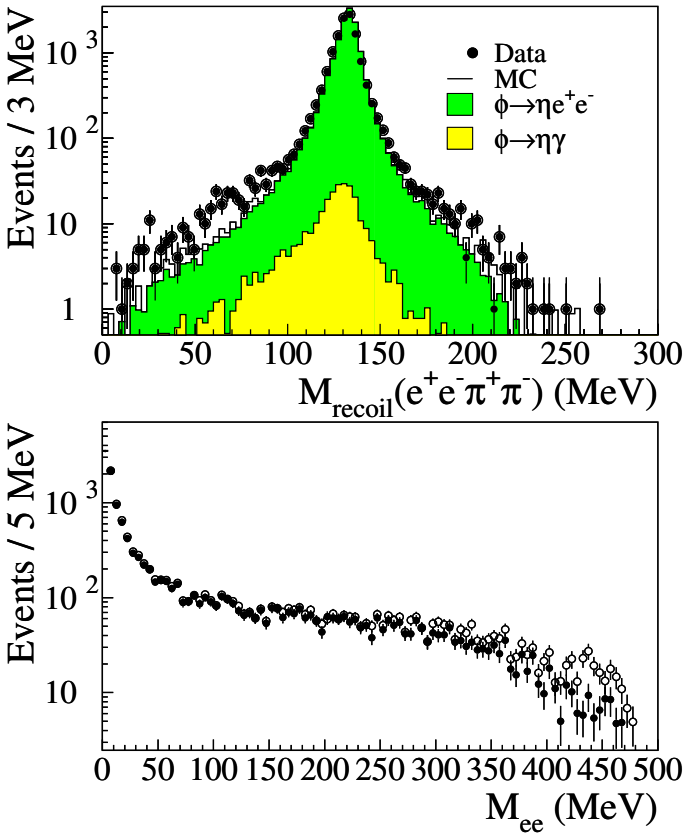

Figure 5: $\phi \to \eta e^+e^-$, $\eta \to \pi^+\pi^-\pi^0$ analysis. Top: data-MC comparison for the recoil mass against the $e^+e^-\pi^+\pi^-$ system. Bottom: M_{ee} distribution before (open circles) and after (black dots) the cut on $M_{\rm recoil}(ee\pi\pi)$.

evaluation is done by summing values over all bins of the two decay channels, taking into account the different luminosity, efficiency and relative branching ratios of the two samples. The systematic error on the background knowledge $\Delta b(M_{ee})$ is evaluated, for each M_U value, changing by one standard deviation the two fit parameters and has been taken into account while evaluating $\mathrm{CL_S}$,

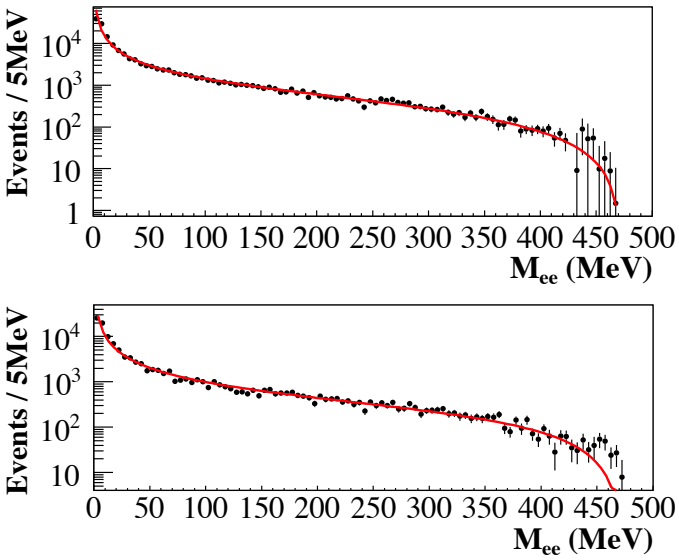

Figure 6: Fit to the corrected M_{ee} spectrum for the Dalitz decays $\phi \to \eta e^+e^-$, with $\eta \to \pi^0\pi^0\pi^0$ (top) and $\eta \to \pi^+\pi^-\pi^0$ (bottom).

applying a Gaussian spread of width $\Delta b(M_{ee})$ on the background distribution. In Fig. 7 top, the upper limit at 90% C.L. on the number of events for the decay chain $\phi \to \eta U$, $U \to e^+e^-$, is shown for both $\eta \to \pi^0\pi^0\pi^0$ and $\eta \to \pi^+\pi^-\pi^0$, separately evaluated. In Fig. 7 bottom, the smoothed upper limit on the branching fraction for the process $\phi \to \eta U$, $U \to e^+e^-$, obtained from the combined method is compared with evaluations from each of the two decay channels. In the combined result, the upper limit on the product $\mathrm{BR}(\phi \to \eta U) \times \mathrm{BR}(U \to e^+e^-)$ varies from 10^{-6} at small M_U to $\sim 3 \times 10^{-8}$ at 450 MeV.

The exclusion plot in the $\alpha'/\alpha = \epsilon^2$ *vs* M_U plane, where α' is the coupling of the U boson to electrons and α is the fine structure constant, has been finally

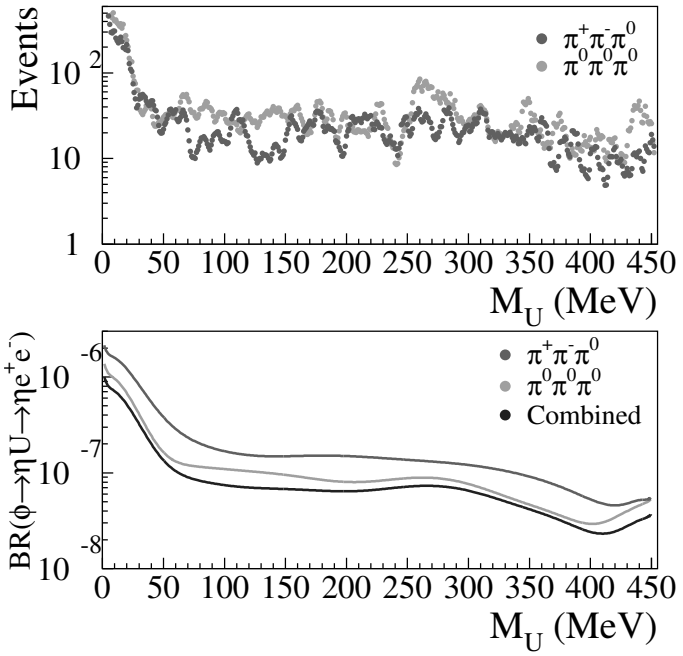

Figure 7: Top: upper limit at 90% C.L. on the number of events for the decay chain $\phi \to \eta U$, $U \to e^+e^-$, with $\eta \to \pi^0\pi^0\pi^0$ and $\eta \to \pi^+\pi^-\pi^0$. Bottom: smoothed upper limit at 90% C.L. on $\mathrm{BR}(\phi \to \eta U) \times \mathrm{BR}(U \to e^+e^-)$, obtained separately for the two η decay channels and from the combined analysis.

derived assuming the relation [10]:

$$\sigma(e^+e^- \to \phi \to \eta U) = \epsilon^2 \, |F_{\phi\eta}(m_U^2)|^2 \, \frac{\lambda^{3/2}(m_\phi^2, m_\eta^2, m_U^2)}{\lambda^{3/2}(m_\phi^2, m_\eta^2, 0)} \, \sigma(e^+e^- \to \phi \to \eta\gamma) \,, \tag{4}$$

with $\lambda(m_1^2, m_2^2, m_3^2) = [1 + m_3^2/(m_1^2 - m_2^2)]^2 - 4m_1^2 m_3^2/(m_1^2 - m_2^2)^2$. We assume that the U boson decays only to lepton pairs, with equal coupling to e^+e^- and $\mu^+\mu^-$.

The extraction of the limit on the α'/α parameter is related to the parametrization of the form factor (Eq. 4), and thus to the Λ parameter in Eq. 3.

The SND experiment measured the form factor slope, $b_{\phi\eta} = dF/dq^2|_{q^2=0} = \Lambda^{-2}$, obtaining $b_{\phi\eta} = (3.8 \pm 1.8)$ GeV^{-2} [14], with a central value different from theoretical predictions based on VMD ($b_{\phi\eta} \sim 1$ GeV^{-2}) [15], although in agreement within the error. In Fig. 8 the smoothed exclusion plot at 90% C.L. on α'/α is compared with existing limits in the same region of interest [16, 17, 18]. The evaluation is done using both the experimental and the theoretical values of the form factor slope. The two resulting curves overlap at low M_{ee} values, while the limit obtained using the SND measurement gives an increasingly larger exclusion region up to ~ 400 MeV, moving closer to the other curve at the end of the phase space.

Having the experimental value of $b_{\phi\eta}$ an uncertainty of $\sim 50\%$, we conservatively use the curve obtained with theoretical predictions, resulting in a limit of: $\alpha'/\alpha < 1.7 \times 10^{-5}$ for $30 < M_U < 400$ MeV, and even better for the sub-region $50 < M_U < 210$ MeV: $\alpha'/\alpha < 8.0 \times 10^{-6}$. Comparing our result with the previous KLOE measurement, reported as the dotted line in Fig. 8, we improve the upper limit of about a factor of two when using the same parametrization of the form factor. This result reduces the region of the U boson parameters that could explain the observed discrepancy between the measurement and Standard Model prediction of the muon anomalous magnetic moment, a_μ, ruling out masses in the range 60–435 MeV.

6 Acknowledgements

We warmly thank our former KLOE colleagues for the access to the data collected during the KLOE data taking campaign. We thank the DAΦNE team for their efforts in maintaining low background running conditions and their collaboration during all data taking. We want to thank our technical staff: G.F. Fortugno and F. Sborzacchi for their dedication in ensuring efficient operation of the KLOE computing facilities; M. Anelli for his continuous attention to the gas system and detector safety; A. Balla, M. Gatta, G. Corradi and G. Papalino for electronics maintenance; M. Santoni, G. Paoluzzi and R. Rosellini for general detector support; C. Piscitelli for his help during major maintenance periods. This work was supported in part by the EU Integrated Infrastructure Initiative Hadron Physics Project under contract number RII3-CT- 2004-506078; by the European Commission under the 7th Framework Programme through the 'Research Infrastructures' action of the 'Capacities' Programme, Call: FP7-

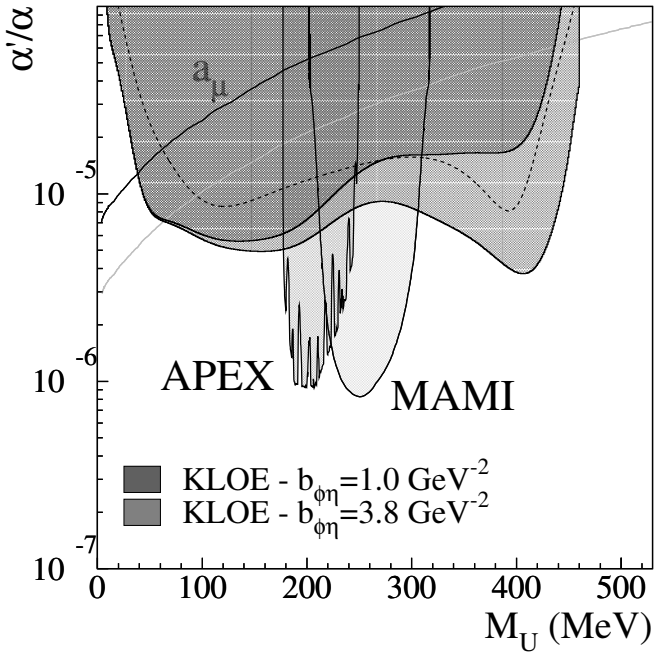

Figure 8: Exclusion plot at 90% C.L. for the parameter $\alpha'/\alpha = \epsilon^2$, compared with existing limits from the muon anomalous magnetic moment and from MAMI/A1 and APEX experiments. The gray line represents the expected values of the U boson parameters needed to explain the observed discrepancy between measured and calculated a_μ values. The dotted line is the previous KLOE result, obtained with the $\eta \to \pi^+\pi^-\pi^0$ channel only.

INFRASTRUCTURES-2008-1, Grant Agreement No. 227431; by the Polish National Science Centre through the Grants No. 0469/B/H03/2009/37, 0309/B/H03/2011/40, DEC-2011/03/N/ST2/02641,
2011/01/D/ST2/00748 and by the Foundation for Polish Science through the MPD programme and the project HOMING PLUS BIS/2011-4/3.

References

1. *An anomalous positron abundance in cosmic rays with energies 1.5−100 GeV*, O. Adriani et al., Nature 458-607 (2009);
2. *Measurement of the Cosmic Ray $e^+ + e^-$ Spectrum from 20 GeV to 1 TeV with the Fermi Large Area Telescope*, A. Abdo et al., Phys. Rev. Lett. 102, 181101 (2009);
3. *Early SPI/INTEGRAL measurements of 511 keV line emission from the 4th quadrant of the Galaxy*, P. Jean et al., Astron. Astrophys. 407, L55 (2003);
4. *Model-independent implications of the $e^{\pm}$, $\bar{p}$ cosmic ray spectra on properties of Dark Matter*, M. Cirelli et al., Nuclear Physics B 813 (2009);
5. M. Adinol et al., Nucl. Inst. and Meth. A 488, 51 (2002);
6. M. Adinolfi et al., Nucl. Inst. and Meth. A 488, 51 (2002).
7. M. Adinolfi et al., Nucl. Inst. and Meth. A 482, 364 (2002).
8. M. Adinolfi et al., Nucl. Inst. and Meth. A 492, 134 (2002).
9. F. Ambrosino et al., Nucl. Inst. and Meth. A 534, 403 (2004).
10. M. Reece, L.T. Wang, JHEP 07, 051 (2009).
11. L.G. Landsberg, Phys. Rep. 128, 301 (1985).
12. F. Archilli et al., Phys. Lett. B 706, 251 (2012).
13. T. Junk, Nucl. Instr. Meth. A 434, 435 (1999).
14. M. N. Achasov et al., Phys. Lett. B 504, 275 (2001).
15. N. N. Achasov and A. A. Kozhevnikov, Sov. J. Nucl. Phys. 55, 449 (1992).
16. H. Merkel et al., Phys. Rev. Lett. 106, 251802 (2011).
17. S. Abrahamyan et al., Phys. Rev. Lett. 107, 191804 (2011).
18. M. Pospelov, Phys. Rev. D 80, 095002 (2009).